Anionic Glycidyl Triazolyl Polymers: Oppositely Charged Analogs of Imidazolium-Based Cationic Glycidyl Triazolyl Polymers

*Taichi Ikeda**

Research Center for Macromolecules and Biomaterials, National Institute for Materials Science, 1-1 Namiki, Tsukuba, Ibaraki, 305-0044, Japan.

ABSTRACT

Glycidyl triazolyl polymer (GTP)-based anionic poly(ionic liquid)s comprising the trifluoromethanesulfonimide (TFSI) anion pendant and the 1-ethyl-3-methylimidazolium (EMIM) counter cation were synthesized through Cu(I)-catalyzed azide-alkyne cycloaddition between a glycidyl azide polymer and anionic alkyne derivatives. These polymers were designed as oppositely charged analogs of the cationic GTPs reported previously. The anionic GTPs were characterized by NMR, IR, size-exclusion chromatography, differential scanning calorimetry, thermogravimetric analysis, and impedance measurements. The anionic GTPs reported herein exhibited lower critical solution temperature (LCST) type phase separation in acetone. The anionic GTPs with a longer side-chain spacer exhibited a lower glass transition temperature (T_g) and higher ionic conductivity (1.7×10^{-6} S cm^{-1} at 25 °C under anhydrous conditions). It was confirmed that the anionic GTPs contains 0.8–0.9 wt% water even after the drying process. It is considered that the residual water contributes to improve the ionic conductivity. Compared to the cationic GTP with a similar side-chain spacer, the anionic GTP exhibited higher T_g and lower ionic conductivity. The analysis based on the electrode polarization model indicated that the lower ionic conductivity would originate from lower conducting ion concentration and mobility. From the conducting ion mobility vs T_g/T plot, it was confirmed that the anionic GTP with the short alkyl chain spacer gave higher conducting ion mobility than that with the ethylene oxide spacer, which suggested that the electrostatic interaction with the ether oxygen atoms could slow down the diffusion of EMIM cation. Stronger electrostatic interaction between the TFSI pendant and EMIM cation than that between the EMIM pendant and TFSI counter ion is a cause of stronger polymer-polymer interaction.

INTRODUCTION

Poly(ionic liquid)s are soft, light-weight and safe (no risk of leakage and fire) electrolytes;[1–4] hence they are promising functional materials in many fields, including energy-storage materials,[5] electrochromic devices,[6] actuators,[7] CO_2 separation,[8] adaptive materials,[9] and stimuli-responsive materials.[10] Owing to their diverse application fields, many research groups continue the quest for new molecular design for modulating the physical properties.[1–4,11–15] In order to elucidate the structure-property relationship of poly(ionic liquid)s, high-molecular-weight poly(ionic liquid)s must be prepared, because their physical properties are strongly dependent on the molecular weight when it is below 10^5 g mol^{-1}.[16] The purity of the polymer is also important, because the impurities, which include the unreacted starting materials, by-products, and solvent, drastically change the physical property.[16] In order to improve ionic conductivity, plasticizer or fillers are often added. These additives can mask the disadvantages of bad molecular design, which leads to controversial conclusions on structure-property relationship. In case of ion-conductive poly(ionic liquid)s, it is often difficult to judge whether high ionic conductivity originates from a good molecular design, low molecular weight of polymer, or impurities. Compared to the polymerization of the ionic liquid monomer, the post-functionalization of the polymer facilitates the preparation of pure and high-molecular-weight poly(ionic liquid)s.[11,17–19] On the basis of these perspectives, cationic glycidyl triazolyl polymers (GTPs) have been synthesized by the post-functionalization of a glycidyl azide polymer (GAP) with alkyne derivatives of ionic liquids via the Cu(I)-catalyzed azide-alkyne cycloaddition (Cu-AAC).[20,21] Owing to the high and selective reactivity of Cu-AAC,[22,23] pure and high-molecular-weight GTPs ($M_w > 10^5$ g mol^{-1}) with different side groups have been systematically synthesized and characterized since 2015.[20] Hence, the cationic GTP with branched side chains was confirmed to break the conventional record of ionic conductivity.[21]

Thus far, only cationic GTPs have been reported. To expand the structural diversity of GTP-based poly(ionic liquid)s, the development of anionic GTPs is awaited. In this study, anionic GTPs comprising the trifluoromethanesulfonimide (TFSI) anion pendant and the 1-ethyl-3-methylimidazolium (EMIM) counter cation were synthesized, which were designed as oppositely charged analogs of the cationic GTPs reported previously (Figure 1).[24] Although the anionic poly(ionic liquid)s with TFSI pendant have been reported by many research groups,[5,7,15,18,19,25] the spacer group between the main chain and the TFSI pendant was always short (-C_3H_6-). In this study, the anionic poly(ionic liquid) with a long flexible spacer was also synthesized (Anionic GTP3). From the ionic conductivities of the anionic GTP2 and GTP3, one can confirm an empirical rule of poly(ionic liquid)s, namely "A long and flexible side-chain spacer renders higher ionic conductivity."[2,16] The anionic GTPs exhibited a unique property that was not observed for the cationic GTPs, i.e., lower critical solution temperature (LCST)-type phase transition in acetone. Some groups reported that the ionic conductivity of anionic poly(ionic liquid)s was higher than that of the cationic analogs.[7,25,26] However, an opposite result was obtained in this study. The objective of this study is to elucidate the reason for ionic conductivity difference between the cationic and anionic GTPs. This issue was discussed on the basis of experimental data of conducting ion concentration and mobility obtained from the electrode polarization (EP) model.[26–29]

(insert Figure 1)

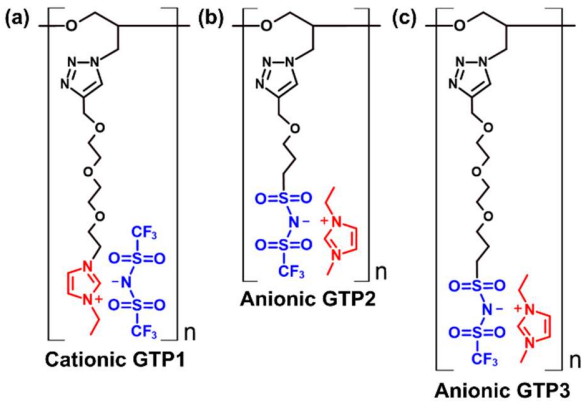

Figure 1. Chemical structures of (a) cationic GTP1 in a previous study.[24] (b)Anionic GTP2 and (c) GTP3 in this study.

EXPERIMENTAL SECTION

Materials. Polyepichlorohydrin (PECH, Average molecular weight: 700 kDa) was purchased from Merck. 2-Propyn-1-ol, 1,3-propanesultone, trifluoromethanesulfonamide, triethylamine (TEA), 1-ethyl-3-methylimidazolium bromide (EMIM·Br), diethylene glycol, propargyl bromide (80% in toluene, ca. 9.2 M), sodium hydride (60%, dispersion in paraffin liquid), potassium *tert*-butoxide, and tetrakis(acetonitrile) copper(I) hexafluorophosphate [$Cu(MeCN)_4 \cdot PF_6$] were purchased from Tokyo Chemical Industry. Thionyl chloride ($SOCl_2$), and distilled water were purchased from Nacalai Tesque. Lithium hydride powder (LiH), and dry solvents were purchased from Kanto Chemical. The metal scavenger (Si-Trisamine) was purchased from Biotage. GAP was prepared from PECH by a procedure reported previously.[20] Compounds **1** and **3** were prepared according to the literatures.[30–32]

Compound 2. Trifluoromethanesulfonamide (2.4 g, 16 mmol) and freshly distilled triethylamine (TEA, 4.6 mL, 33 mmol) were dissolved in dry THF (10 mL) under N_2 atmosphere. To this solution, the compound **1** (3.2 g, 16 mmol) in dry THF (10 mL) was added slowly with a syringe. The reaction mixture was allowed to react at 20 ºC for 2 h. After the filtration, the solvent was removed by evaporation. The residue was dissolved in CH_2Cl_2 (80 mL), then washed with distilled water (10 mL) in four times. The organic layer was recovered, dried with $MgSO_4$, and filtrated. The solvent was removed by evaporation. The recovered product (5.5 g, 13 mmol) was dissolved in dry THF (10 mL) under N_2 atmosphere. To this solution, lithium hydride (0.26 g, 33 mmol) was added. The reaction mixture was allowed to react at 25 ºC overnight. After the filtration, the solvent was removed by evaporation. The residue was washed with hexane (50 mL × 2). The residue was dissolved in distilled water (80 mL), then washed with diethyl ether (10 mL) in four times. After the treatment with activated carbon (1 g), water was removed by evaporation. The residue was dissolved in dichloromethane/methanol (9/1, v/v), dried with $MgSO_4$, and filtrated. The solvent was removed by evaporation. The recovered product (4.1 g, 13 mmol) was dissolved in distilled water (10 mL). 1-Ethyl-3-methylimidazolium bromide (5.0 g, 26 mmol) dissolved in distilled water (10 mL) was added. The reaction mixture was allowed to react at 20 ºC for 1h. After concentration by evaporation, the product was extracted with CH_2Cl_2 (80 mL), then it was washed with distilled water (10 mL) in three times. The organic layer was dried with $MgSO_4$, and filtrated. The solvent was removed by evaporation to give the product as pale-yellow liquid. Yield: 3.9 g (57 %). ^{1}H NMR (400 MHz, $CDCl_3$): δ = 1.54 (t, J = 7.4 Hz, 3H), 2.12 (m, 2H), 2.43 (t, J = 2.4 Hz, 1H), 3.22 (m, 2H), 3.62 (t, J = 6.2 Hz, 2H), 3.96 (s, 3H), 4.11 (d, J = 2.4 Hz, 2H), 4.27 (q, J = 7.4 Hz, 2H), 7.34 (br, 2H), 9.09 (s, 1H); ^{13}C NMR (100 MHz, $CDCl_3$): δ = 15.4, 24.5, 36.5, 45.3, 52.4, 58.2, 68.2, 74.6, 79.8, 120.4 (q, J = 321 Hz), 121.9, 123.7, 136.7.

Compound 4. Compound **3** (5.8 g, 20 mmol) and thionyl chloride (10 mL, 0.14 mol) were allowed to react at 60 ºC for 3h under N_2 atmosphere. Thionyl chloride was removed by distillation under reduced pressure at 45 ºC. After adding toluene (10 mL), the solvent was removed by distillation under reduced pressure at 50 ºC. After adding dichloromethane, the insoluble salt was removed by filtration. The filtrate was concentrated by evaporation. The residue was purified by column chromatography (SiO_2, hexane/ethyl acetate/acetone = 7/2/1). Yield: 4.5 g (78 %). ^{1}H NMR (400 MHz, $CDCl_3$): δ = 2.30 (m, 2H), 2.44 (t, J = 2.4 Hz, 1H), 3.60–3.72 (m, 10H), 3.84 (m, 2H), 4.20 (d, J = 2.4 Hz, 2H); ^{13}C NMR (100 MHz, $CDCl_3$): δ = 25.3, 58.7, 63.0, 68.0, 69.4, 70.6, 70.8, 70.9, 75.0, 79.9.

Compound 5. The synthetic procedures were the same as the compound **2**. Yield: 2.9 g (54 %). ^{1}H NMR (400 MHz, $CDCl_3$): δ = 1.54 (t, J = 7.4 Hz, 3H), 2.09 (m, 2H), 2.44 (t, J = 2.4 Hz, 1H), 3.20 (m, 2H), 3.54–3.71 (m, 10H), 3.97 (s, 3H), 4.17 (d, J = 2.4 Hz, 2H), 4.28 (q, J = 7.4 Hz), 7.34 (d, J = 2.0 Hz, 2H), 9.12 (s, 1H); ^{13}C NMR (100 MHz, $CDCl_3$): δ = 15.4, 24.6, 36.5, 45.3, 52.4, 58.5, 69.2, 69.4, 70.2, 70.5, 70.7, 74.8, 79.7, 120.4 (t, J = 321 Hz), 121.8, 123.7, 136.8.

Anionic GTP2. GAP (0.20 g, 2.0 mmol monomer unit) was dissolved completely in dry DMF (10 mL) with stirring at 50 ºC. (Caution: Never heat up too much and never agitate by sonication.) After adding the compound **2** (1.2 g, 2.9 mmol), the solution was purged with N_2, then the copper catalyst ($Cu(MeCN)_4 \cdot PF_6$, 80 mg, 0.21 mmol) was added. The mixture was stirred at 60 ºC under N_2 atmosphere for 24 h. After cooling to room temperature, the solution was treated with the metal scavenger (Si-Trisamine, 1.0 g × 2) for 30 min under air. After the filtration, the solution was concentrated by evaporation. The solution was added dropwise to diethyl ether (200 mL) with stirring to precipitate the product. After 30 min, the solvent was removed by decantation. The precipitate was dissolved in acetone (100 mL). The solution was concentrated by evaporation. The

solution was added dropwise to dichloromethane (300 mL) with stirring to precipitate the product. After 30 min, the solvent was removed by decantation. The product was dissolved in acetone (100 mL), then the solvent was completely removed by evaporation. The product attached on the wall of flask was washed with dichloromethane with stirring for 20 min, then the solvent was removed by decantation. The solvent was completely removed under vacuum (< 0.1 mbar) at 100 ºC for 16 h. Yield: 0.85 g (81%). ^{1}H NMR (400 MHz, CD_3CN): δ = 1.43 (t, J = 7.4 Hz, 3H), 1.9–1.98 (overlapping to solvent peak), 3.05 (br, 2H), 3.27–3.52 (br, 2H), 3.53 (br, 2H), 3.68–3.80 (br, 1H), 3.82 (s, 3H), 4.17 (q, J = 7.4 Hz, 2H), 4.22–4.47 (br, 2H), 4.50 (s, 2H), 7.37 (d, J = 1.6 Hz, 1H), 7.42 (d, J = 1.6 Hz, 1H), 7.85 (br, 1H), 8.57 (s, 1H); ^{13}C NMR (100 MHz, CD_3CN): δ = 15.6, 25.5, 36.8, 45.8, 51.7, 53.2, 64.5, 69.1, 69.7, 78.7, 121.5 (q, J = 321 Hz), 123.0, 124.7, 125.8, 136.9, 145.5.

Anionic GTP3. The synthetic procedures were the same as the anionic GTP2. Yield: 0.94 g (77%). ^{1}H NMR (400 MHz, CD_3CN): δ = 1.44 (t, J = 7.4 Hz, 3H), 1.9–1.98 (overlapping to solvent peak), 3.06 (br, 2H), 3.35 (br, 1H), 3.42–3.60 (br, 9H), 3.75 (br, 1H), 3.83 (s, 3H), 4.17 (q, J = 7.4 Hz, 2H), 4.22–4.48 (br, 2H), 4.54 (s, 2H), 7.37 (d, J = 1.6 Hz, 1H), 7.42 (d, J = 1.6 Hz, 1H), 7.85 (br, 1H), 8.57 (s, 1H); ^{13}C NMR (100 MHz, CD_3CN): δ = 15.6, 25.5, 36.8, 45.8, 51.7, 53.1, 64.7, 69.8, 70.3, 70.7, 71.0, 71.0, 78.6, 121.5 (q, J = 321 Hz), 123.0, 124.7, 125.8, 136.9, 145.4.

(insert Scheme 1)

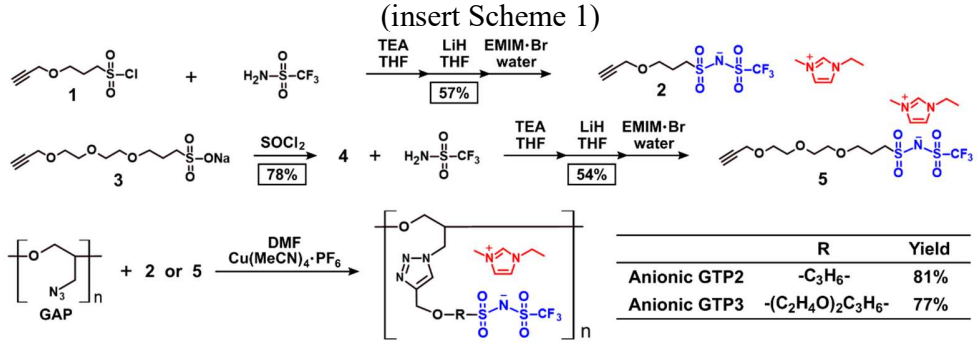

	R	Yield
Anionic GTP2	-C_3H_6-	81%
Anionic GTP3	-$(C_2H_4O)_2C_3H_6$-	77%

Scheme 1. Synthetic scheme of anionic GTPs.

RESULTS AND DISCUSSION

Synthesis of anionic GTPs. Scheme 1 shows the synthetic scheme of the anionic alkyne derivatives and anionic GTPs. The TFSI group was introduced by the reaction between the sulfonyl chloride derivatives (compounds **1** and **4**) and trifluoromethanesulfonamide. After the counter-ion metathesis,[5,33] the anionic alkyne derivatives (compounds **2** and **5**) were obtained. The ^{1}H and ^{13}C NMR spectra of the compounds **1**–**5** are shown in Figures S1–S5. The anionic GTPs were synthesized by the Cu-AAC reaction between GAP and the anionic alkyne derivatives. As a model polymer, a non-ionic GTP (GTP-Bz) was also synthesized.[34] Notably, all of the GTPs were prepared from the same GAP sample. After the Cu-AAC reaction, the metal scavenger was used to remove the copper catalyst. Quantitative functionalization was confirmed by the disappearance of the azide peak in the IR spectrum (Figure S11, ν = 2100 cm^{-1}). GTPs were recovered by precipitation in a poor solvent. As a part of GTP was lost during the work-up process, the recovered yields of the products were approximately 80%.

The chemical structures of the anionic GTPs were confirmed by ^{1}H and ^{13}C NMR measurements. Figures 2a and 2b show the ^{1}H NMR and ^{13}C NMR spectra of anionic GTP3, respectively. All of the peaks were assigned by heteronuclear multiple quantum correlation (HMQC) and heteronuclear multiple bond coherence (HMBC) experiments (Figures S8 and S9). The glycidyl protons (a, b, and c) exhibited broad peaks due to a shorter relaxation time, reflecting lower main-chain mobility. On the contrary, the EMIM protons (red color in Figure 2a) exhibited sharp peaks due to the higher mobility of the counter cation. The integrals of the peaks proved 1:1 ratio of the repeating unit and the counter ion (see the triazole proton d and imidazolium protons l, m and n in Figure S7). In the ^{13}C NMR spectrum, all of the carbon peaks assigned to the glycidyl main chain, triazole group (green), ethylene glycol and methylene spacer, TFSI group (blue), and EMIM cation

(red) were detected. The trifluoromethyl carbon exhibited typical quartet peaks at 121.5 ppm (coupling constant: 321 Hz, blue color peaks marked * in Figure 2b). Notably, peaks corresponding to the solvent (except for the NMR solvent of MeCN and water) and impurities were not observed. From the integral value of water peak, the water content in the sample was calculated (Figure S10). When the sample was stored under the laboratory condition (under air, room temperature, no humidity control), the anionic GTP3 contains one water molecule per repeating unit (2.9 wt% water content, Figure S10b). When the anionic GTP3 was dried at 120 ºC for 2 h under dry N_2 flow, the water content decreased to *ca*. 0.9 wt% (Figure S10c). Even if the anionic GTP3 was dried under more severe condition (120 ºC, < 0.1 mbar, 16 h), the water content did not decrease below 0.9 wt% (Figure S10d). This result indicates that some water molecules are strongly bound to the polymer and cannot be removed. The water content of the anionic GTP2 after drying (120 ºC, 2 h, dry N_2 flow) was *ca*. 0.8 wt% (Figure S10e). It is considered that the hydrophilic groups in the chemical structure of GTP (polyether main chain and triazole group) contribute to keep the water molecules.

(insert Figure 2)

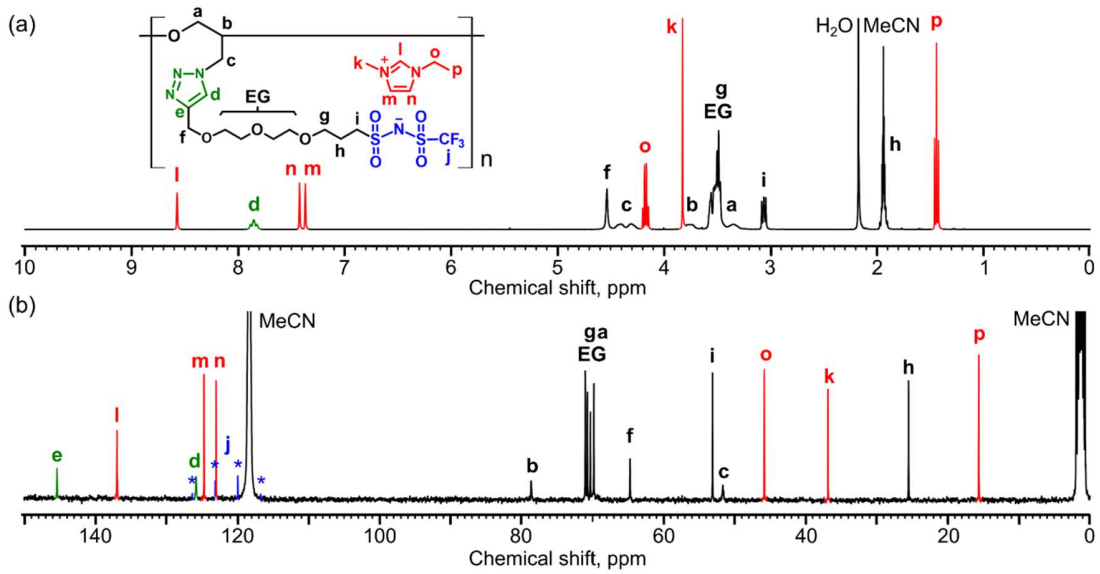

Figure 2. (a) ^{1}H NMR and (b) ^{13}C NMR spectra of anionic GTP3. Assignment of each peak is also depicted.

The molecular weight of the anionic GTP was determined using the non-ionic model GTP (GTP-Bz) because the anionic GTP did not exhibit a peak in the GPC curve presumably because of its adsorption on the column resin (Figure S12). The number-average and weight-average molecular weights (M_n and M_w) of GTP-Bz were 3.06×10^5 and 7.19×10^5 g mol^{-1}, respectively (Polystyrene standard). The molecular weight of GTP-Bz was considerably less than that expected from the molecular weight of the starting material PECH ($M_w = 7 \times 10^5$ g mol^{-1}) because of the decrease in the molecular weight during the azidation reaction.[20,34] The M_n and M_w values of the anionic GTPs were calculated from the degree of polymerization of GTP-Bz (Table 1). The molecular weights of the anionic GTPs were comparable to those of the cationic GTPs reported previously.[24]

(insert Table 1)

Table 1. Molecular weights and thermal properties.

Sample name	M_n(g mol^{-1}) [a]	M_w(g mol^{-1}) [b]	T_g(°C) [c]	T_{d5}(°C)[d]
Compound **2**	419.4	–	−70	–
Compound **5**	507.5	–	−61	–
GTP-Bz	3.06×10^5	7.19×10^5	60[e]	342[e]
Cationic GTP1[f]	6.37×10^5	1.28×10^6	−31	347
Anionic GTP2	7.37×10^5 [g]	1.73×10^6 [g]	−10	317
Anionic GTP3	8.63×10^5 [g]	2.03×10^6 [g]	−25	329

[a]Number-average molecular weight. [b]Weight-average molecular weight. [c]Glass transition temperature (DSC onset value during heating). [d]5% weight loss temperature according to TGA performed under inert atmosphere. [e]Data from reference 34. [f] Data from reference 24. [g]Molecular weight was calculated from the degree of polymerization of the model polymer GTP-Bz.

Solution property of anionic GTPs. The anionic GTPs were soluble in aprotic polar solvents such as acetone, MeCN, DMF, and dimethyl sulfoxide. In contrast, the anionic GTPs were insoluble in water and nonpolar solvents such as hexane, diethyl ether, and dichloromethane. Anionic GTP2 and GTP3 exhibited LCST-type phase separation in acetone. During the heating process of the anionic GTP2 solution, the transmittance dropped at a temperature higher than 53 °C (Figure 3a). The soluble and insoluble states of anionic GTP2 were shown in the inset photos (Figures 3d and 3e). Hysteresis was observed in the heating and cooling processes. During the heating process of the anionic GTP3 solution, transmittance did not drop up to the boiling point of acetone (56 °C), which suggests that the cloud appearance (Figure 3e) and the transmittance drop of the GTP2 solution (Figure 3a) does not originate from the bubbles generated by acetone boiling. When the sample cell of the GTP3 solution was heated using a heat gun, the phase transition could be induced (Figure S13). Gradual heating using a sample cell holder in a spectrometer cannot render a temperature higher than the boiling point of acetone due to evaporative cooling. On the

other hand, rapid heating using a heat gun can be the sample cell wall temperature above 56 °C. Several research groups have reported poly(ionic liquid)s exhibiting LCST-type phase separation.[10,35–37] However, this is the first example of LCST poly(ionic liquid)s comprising the TFSI pendant and imidazolium counter cation. The LCST-type phase separation was not observed for the cationic GTPs. These results suggested that the polymer-polymer interaction of the anionic GTPs reported herein was larger than that of the cationic GTPs reported previously.

(insert Figure 3)

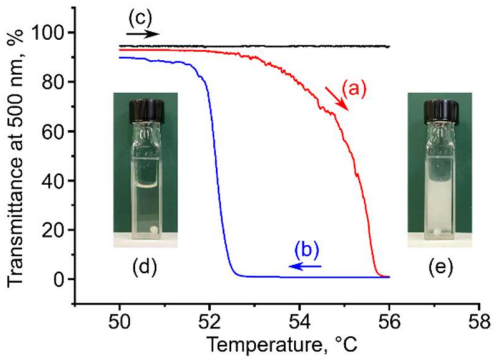

Figure 3. Temperature-dependent transmittance changes (4 wt% polymer in acetone, heating and cooling rates: ±0.1 ºC min^{-1}). (a) Heating process of anionic GTP2. (b) Cooling process of anionic GTP2. (c) Heating process of anionic GTP3. Inset photos. (d) Soluble state of anionic GTP2. White stirring bar is shown at the bottom. (e) Insoluble state of anionic GTP2. Polymer at bottom started to dissolve during taking the photo.

Thermal properties. Thermal properties were characterized by DSC. Figure S14 and Table 1 summarize the results. In these DSC charts, only one glass transition temperature (T_g) was observed and no melting or crystallization peaks were observed, indicating the sample is amorphous and there is no phase separation or significant heterogeneity in the samples.

Compounds **2** and **5** exhibited glass transition at −70 °C and −61 °C, respectively. These anionic alkyne derivatives were liquids at room temperature; therefore, they are ionic liquids. The T_g of **5** was higher than that of **2** (Table 1). On the contrary, the T_g values of anionic GTP3 prepared from the compound **5** (−25 °C) was lower than that of anionic GTP2 prepared from the compound **2** (−10 °C). The long and flexible side chains are considered to increase the polymer segmental mobility. The T_g value of anionic GTP3 was higher than that of cationic GTP1 (−31 °C), even though both GTPs have similar side-chain spacer length.[24] As mentioned above in the result of LCST-type phase separation, this result also suggested that the polymer-polymer interaction of anionic GTP was larger than that of cationic GTP.

The thermal decomposition behavior of the anionic GTPs was investigated by TGA. The sample weight decreased ca. 2.0 % during the heating to 250 ºC. This result is consistent to the water content change before and after the drying process (see above). Figure S15 and Table 1 summarize the TGA results. The 5 wt% decomposition temperature (T_{d5}) was higher than 300 °C. Compared with those of the cationic GTPs, the T_{d5} values of the anionic GTPs were slightly lower. However, the anionic GTPs exhibited sufficient thermal stability to conduct impedance measurements at temperatures between 10 °C and 100 °C.

Ionic conductivity. The ionic conductivities of the anionic GTPs were analyzed by impedance spectroscopy under anhydrous condition. Before impedance measurement, the sample was dried at 120 ºC for 2 h under dry N_2 flow. As discussed above, the anionic GTP2 and GTP3 contain 0.8 wt% and 0.9 wt% water, respectively. Since the amount of the residual water does not change after the drying process, ionic conductivity of the anionic GTP2 and GTP3 reported herein are reproducible, which was confirmed by the measurements in three times. The direct current

conductivity (σ_{DC}, S cm^{-1}) is the product of charge (e = 1.60 × 10^{-19} C), conducting ion concentration (p, cm^{-3}), and conducting ion mobility (μ, cm^2 V^{-1}s^{-1}).

$$\sigma_{DC} = e \cdot p \cdot \mu \qquad (1)$$

The p and μ values were obtained from the EP model analysis (Supporting Information).[21,24,26–29] Figure 4 and Tables S1–S6 summarize the data (σ_{DC}, p and μ). The p values of the anionic GTPs are on the order of 10^{17} (cm^{-3}), whereas the bulk concentrations of EMIM$^+$ counter ion are on the order of 10^{21} (cm^{-3}), which were calculated by assuming the anionic GTP density to be 1.4 g cm^{-3}. This result indicates that the conducting ion content is on the order of 0.1 %, which is comparable to the values for single-ion conducting polyelectrolytes.[21,24,29] On the other hand, A.P. Sokolov *et al.* reported the inverse Haven ratio around 0.1 for single-ion conducting polyelectrolytes, indicating ca. 10 % conducting ion content.[38] It should be noted that the diffusion constant calculated from the impedance measurement differs depend on the applied model.[39] For comparing the data reported herein to those in our previous study, the EP model was applied in this study. The σ_{DC} and μ values followed the Vogel–Fulcher–Tammann (VFT)-type temperature dependence, reflecting the coupling with the segmental motion of the polymer matrix. The p value followed the Arrhenius-type temperature dependence with the activation energy (E_a).

$$\sigma_{DC} = \sigma_0 \times \exp\{-B_\sigma/(T - T_{\sigma 0})\} \qquad (2)$$

$$p = p_0 \times \exp(-E_a/RT) \qquad (3)$$

$$\mu = \mu_0 \times \exp\{-B_\mu/(T - T_{\mu 0})\} \qquad (4)$$

where σ_0, p_0, μ_0, B_σ, B_μ, $T_{\sigma 0}$, and $T_{\mu 0}$ are the constants.[24] Table 2 summarizes the σ_{DC}, p, and μ values at 25 °C.

(insert Figure 4)

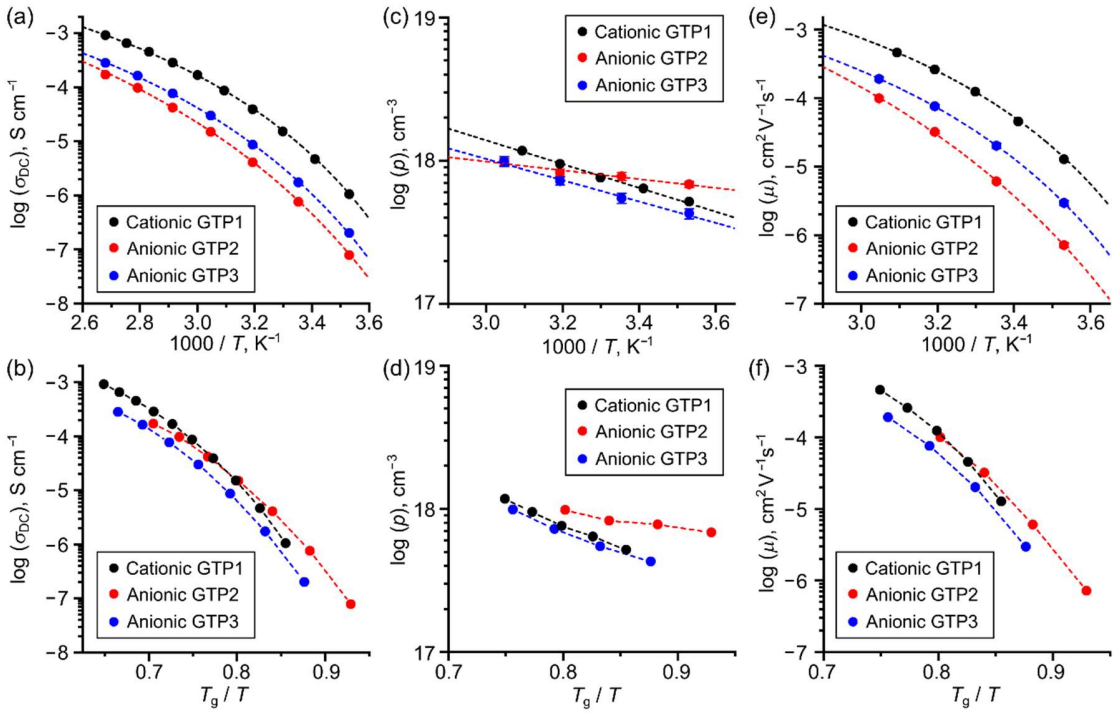

Figure 4. Temperature dependence of (a) DC conductivity (σ_{DC}). Dashed curves were fitted using equation (2). (b) σ_{DC} vs T_g/T plot. (c) Conducting ion concentration (p). Dashed curves were fitted using equation (3). (d) p vs T_g/T plot. (e) Conducting ion mobility (μ). Dashed curves were fitted using equation (4). μ vs T_g/T plot. All measurements were conducted under anhydrous condition.

(insert Table 2)

Table 2. Ionic conductivity data of GTPs at 25 ºC under anhydrous condition.[a]

Sample name	σ_{DC} (S cm^{-1})[b]	p (cm^{-3})[c]	μ (cm^2 V^{-1}s^{-1})[d]
Anionic GTP2	7.5×10^{-7}	7.8×10^{17}	6.0×10^{-6}
Anionic GTP3	1.7×10^{-6}	5.5×10^{17}	2.0×10^{-5}

[a]Although impedance measurement was conducted under anhydrous condition (dry N_2 atmosphere), the anionic GTP2 and GTP3 contain *ca*. 0.8 wt% and 0.9 wt% water, respectively. [b]DC conductivity under anhydrous condition. [c]Conducting ion concentration obtained by EP model analysis. [d]Conducting ion mobility obtained by EP model analysis.

The σ_{DC} value of anionic GTP3 at 25 °C (1.7×10^{-6} S cm^{-1}) was higher than that of anionic GTP2 (7.5×10^{-7} S cm^{-1}). This result followed an empirical rule of poly(ionic liquid)s, namely "A long and flexible side-chain spacer renders higher ionic conductivity."[2,16] The ionic conductivity of anionic GTP3 was one-order higher than that reported for the polymethylmethacrylate (PMMA)-based anionic poly(ionic liquid)s comprising the TFSI pendant and imidazolium counter cation (1.5×10^{-7} S cm^{-1} at 25 °C),[7] which supports the superiority of the molecular design for the anionic GTP3. It is considered that the residual water in the anionic GTP also contributes better ionic conductivity than the PMMA-based analogues. The σ_{DC} value of anionic GTP3 was considerably less than that of cationic GTP1 despite the similar side-chain spacer length (Figure 4a). When the σ_{DC} values were plotted against T_g/T, the gap of the σ_{DC} values became small, but it still existed (Figure 4b). Some groups have reported an opposite trend that the anionic poly(ionic liquid) renders higher ionic conductivity than the cationic analog.[7,25,26] The results of the EP model analysis indicated that the lower ionic conductivity of anionic GTP3 than that of cationic GTP1 originated from the lower p and μ values (Figures 4c and 4e). The carriers of ionic conduction for the cationic GTP and anionic GTP were the TFSI counter anion and EMIM counter cation, respectively. The diffusion of the ion in the polymer matrix is affected by both the

electrostatic interaction and the elastic force of the polymer matrix (segmental motion).[38] In case of the poly(ethylene oxide) (PEO)–salt complex electrolyte, a small cation such as Li^+ could be strongly entrapped by the surrounding ether oxygen groups via electrostatic interactions; thus, the diffusion of the cation is slower than that of the anion.[38,40] On the other hand, it was reported that the diffusion of the EMIM cation was faster than that of the TFSI anion in PEO because the diffusion of the large cation is affected by the elastic force of the polymer matrix more significantly.[40] Taking van der Waals radii of EMIM cation and TFSI anion (0.303 nm and 0.329 nm, respectively) into account,[41] this result seems to be reasonable. However, it should be noted that the ion association also affects the ion diffusion.[42] In cases of poly(ionic liquid)s, the associated ions cannot be the mobile ion because one of the ions (cation or anion) is anchored to the polymer chain. Therefore, the ion association does not change the conducting ion mobility, but it does reduce the conducting ion concentration in poly(ionic liquid)s. The T_g/T plot can eliminate the difference arising from the effect of the segmental motion and highlight the effect of the electrostatic force. The μ values of anionic GTP2 were larger than those of GTP3 in the T_g/T plot (Figure 4f). This result suggested that electrostatic interaction with the ether oxygen groups of the side chain spacer could slow down the diffusion of the EMIM cation. Because the anionic poly(ionic liquid)s reported by the other groups were designed without the polyether spacer, it is considered that those gave higher ionic conductivity than the cationic analogs.[7,25,26]

The electrostatic interaction between the TFSI pendant and EMIM counter ion must be larger than that between the EMIM pendant and TFSI counter ion, because the anionic charge of the TFSI pendant was less delocalized by only one trifluoromethyl (CF_3) group. The lower p value of anionic GTP3 than that of cationic GTP1 also suggested stronger electrostatic interactions between the TFSI pendant and EMIM counter ion (Figure 4d). This is a plausible explanation for larger elastic

force (lower segmental motion) of anionic GTP3 than cationic GTP1. The stronger electrostatic interaction between the polymers might also link to LCST behavior of anionic GTPs.

In the ionic conductivity vs T_g/T plot, the ionic conductivity of anionic GTP2 was comparable to that of anionic GTP3 at higher temperatures, but it became larger and exceeds over the values of cationic GTP1 at lower temperatures (Figure 4b). This result originated from the higher p value of anionic GTP2 at low temperatures (Figure 4d). A similar trend that GTP with a short alkyl-chain spacer gave higher p value than that with an oligo(ethylene glycol) spacer was reported for the cationic GTPs (Figure S17).[43] Presumably, a short alkyl chain might suppress the ion association due to the restricted degree of freedom of the ionic pendant group.

CONCLUSION

The anionic GTPs comprising the TFSI anion pendant and the EMIM counter cation were successfully synthesized. The anionic GTPs reported herein exhibited LCST-type phase separation in acetone. The LCST-behavior has not been reported for the cationic GTP analogs. It was considered that strong electrostatic interactions between the polymers link to LCST behavior of anionic GTPs. The anionic GTPs reported herein showed higher ionic conductivity than the PMMA-based analogues. It was confirmed that the anionic GTPs contains 0.8–0.9 wt% water even after the drying process. It is considered that the hydrophilic groups in the chemical structure of GTP (polyether main chain and triazole group) contribute to keep the water molecules. The residual water in the anionic GTP might contribute to improve the ionic conductivity. The anionic GTPs with a longer side-chain spacer exhibited a lower T_g and higher ionic conductivity. Compared to cationic GTP1, anionic GTP3 exhibited a higher T_g and lower ionic conductivity despite of the similar side-chain spacer length. The results of EP analysis indicated that the lower

ionic conductivity originated from lower p and μ values. It was considered that the diffusion of the EMIM cation slows down by two factors. The first factor is the electrostatic interaction between the EMIM cation and the ether oxygen groups of the side chain spacer, which contributes to lower segmental motion at the same time. The second factor is larger elastic force (lower segmental motion) of the polymer matrix based on larger electrostatic interaction between the TFSI pendant and the EMIM cation, which contributes to lower conducting ion concentration at the same time. As a consequence, anionic GTPs reported herein exhibited higher T_g and lower ionic conductivity than those of cationic GTP analogs.

ASSOCIATED CONTENT

Supporting Information.

The Supporting Information is available free of charge at https://pubs.acs.orh/doi.

Additional Figures and Tables: NMR spectra, water content measurement, IR spectra, SEC traces, LCST behavior of anionic GTP3 in acetone, Details on EP model analysis and Impedance data (PDF).

AUTHOR INFORMATION

Corresponding Author

Taichi Ikeda – *Research Center for Macromolecules and Biomaterials, National Institute for Materials Science, Tsukuba, Ibaraki 305-0044, Japan*; orcid.org/0000-0001-6650-5798; E-mail: IKEDA.Taichi@nims.go.jp

Notes

The author declares no competing financial interest.

ACKNOWLEDGMENT

This work was financially supported by Grant-in-Aids for Scientific Research C, 22K05246 (JSPS).

REFERENCES

(1) Yuan, J. Y.; Mecerreyes, D.; Antonietti, M. Poly(Ionic Liquid)s: An Update. *Prog. Polym. Sci.* **2013**, *38,* 1009–1036.

(2) Nishimura, N.; Ohno, H. 15th Anniversary of Polymerised Ionic Liquids. *Polymer* **2014**, *55,* 3289–3297.

(3) Qian, W. J.; Texter, J.; Yan, F. Frontiers in Poly(Ionic Liquid)s: Syntheses and Applications. *Chem. Soc. Rev.* **2017**, *46,* 1124–1159.

(4) Zhang, S. Y.; Zhuang, Q.; Zhang, M.; Wang, H.; Gao, Z. M.; Sun, J. K.; Yuan, J. Y. Poly(Ionic Liquid) Composites. *Chem. Soc. Rev.* **2020**, *49,* 1726–1755.

(5) Porcarelli, L.; Shaplov, A. S.; Salsamendi, M.; Nair, J. R.; Vygodskii, Y. S.; Mecerreyes, D.; Gerbaldi, C. Single-Ion Block Copoly(Ionic Liquid)s as Electrolytes for All-Solid State Lithium Batteries. *ACS Appl. Mater. Interfaces* **2016**, *8,* 10350–10359.

(6) Yang, B. G.; Yang, G. J.; Zhang, Y. M.; Zhang, S. X. A. Recent Advances in Poly(Ionic Liquid)s for Electrochromic Devices. *J. Mater. Chem. C* **2021**, *9,* 4730–4741.

(7) Kokubo, H.; Sano, R.; Murai, K.; Ishii, S.; Watanabe, M. Ionic Polymer Actuators Using Poly(Ionic Liquid) Electrolytes. *Eur. Polym. J.* **2018**, *106,* 266–272.

(8) Bernardo, G.; Gaspar, H. Recent Advances in Poly(Ionic Liquid)-Based Membranes for CO_2 Separation. *Polymers* **2023**, *15*, 667.

(9) Potaufeux, J. E.; Odent, J.; Notta-Cuvier, D.; Lauro, F.; Raquez, J. M. A Comprehensive Review of the Structures and Properties of Ionic Polymeric Materials. *Polym. Chem.* **2020**, *11,* 5914–5936.

(10) Banerjee, P.; Anas, M.; Jana, S.; Mandal, T. K. Recent Developments in Stimuli-Responsive Poly(Ionic Liquid)s. *J. Polym. Res.* **2020**, *27*, 177.

(11) Jourdain, A.; Serghei, A.; Drockenmuller, E. Enhanced Ionic Conductivity of a 1,2,3-Triazolium-Based Poly(Siloxane Ionic Liquid) Homopolymer. *ACS Macro Lett.* **2016**, *5,* 1283–1286.

(12) Guzman-Gonzalez, G.; Vauthier, S.; Alvarez-Tirado, M.; Cotte, S.; Castro, L.; Gueguen, A.; Casado, N.; Mecerreyes, D. Single-Ion Lithium Conducting Polymers with High Ionic Conductivity Based on Borate Pendant Groups. *Angew. Chem. Int. Ed.* **2022**, *61*, e202114024.

(13) Jones, S. D.; Nguyen, H.; Richardson, P. M.; Chen, Y. Q.; Wyckoff, K. E.; Hawker, C. J.; Clement, R. J.; Fredrickson, G. H.; Segalman, R. A. Design of Polymeric Zwitterionic Solid Electrolytes with Superionic Lithium Transport. *ACS Cent. Sci.* **2022**, *8,* 169–175.

(14) Hu, H.; Wang, B. S.; Chen, B. H.; Deng, X.; Gao, G. H. Swellable Poly(Ionic Liquid)s: Synthesis, Structure-Property Relationships and Applications. *Prog. Polym. Sci.* **2022**, *134*, 101607.

(15) Nosov, D. R.; Ronnasi, B.; Lozinskaya, E. I.; Ponkratov, D. O.; Puchot, L.; Grysan, P.; Schmidt, D. F.; Lessard, B. H.; Shaplov, A. S. Mechanically Robust Poly(Ionic Liquid) Block Copolymers as Self-Assembling Gating Materials for Single-Walled Carbon-Nanotube-Based Thin-Film Transistors. *ACS Appl. Polym. Mater.* **2023**, *5,* 2639–2653.

(16) Shaplov, A. S.; Lozinskaya, E. I.; Ponkratov, D. O.; Malyshkina, I. A.; Vidal, F.; Aubert, P. H.; Okatova, O. V.; Pavlov, G. M.; Komarova, L. I.; Wandrey, C.; Vygodskii, Y. S. Bis(Trifluoromethylsulfonyl)Amide Based "Polymeric Ionic Liquids": Synthesis, Purification and Peculiarities of Structure-Properties Relationships. *Electrochim. Acta* **2011**, *57,* 74–90.

(17) Hu, H. Y.; Yuan, W.; Jia, Z.; Baker, G. L. Ionic Liquid-Based Random Copolymers: A New Type of Polymer Electrolyte with Low Glass Transition Temperature. *RSC Adv.* **2015**, *5,* 3135–3140.

(18) Ho, H. T.; Tintaru, A.; Rollet, M.; Gigmes, D.; Phan, T. N. T. A Post-Polymerization Functionalization Strategy for the Synthesis of Sulfonyl (Trifluoromethanesulfonyl)Imide Functionalized (Co)Polymers. *Polym. Chem.* **2017**, *8,* 5660–5665.

(19) Hatakeyama-Sato, K.; Kimura, S.; Matsumoto, S.; Oyaizu, K. Facile Synthesis of Poly(Glycidyl Ether)s with Ionic Pendant Groups by Thiol-Ene Reactions. *Macromol. Rapid Commun.* **2020**, *41*, 1900399.

(20) Ikeda, T. Glycidyl Triazolyl Polymers: Poly(Ethylene Glycol) Derivatives Functionalized by Azide-Alkyne Cycloaddition Reaction. *Macromol. Rapid Commun.* **2018**, *39*, 1700825.

(21) Ikeda, T. Poly(Ionic Liquid)s with Branched Side Chains: Polymer Design for Breaking the Conventional Record of Ionic Conductivity. *Polym. Chem.* **2021**, *12,* 711–718.

(22) Rostovtsev, V. V.; Green, L. G.; Fokin, V. V.; Sharpless, K. B. A Stepwise Huisgen Cycloaddition Process: Copper(I)-Catalyzed Regioselective "Ligation" of Azides and Terminal Alkynes. *Angew. Chem. Int. Ed.* **2002**, *41,* 2596–2599.

(23) Meldal, M.; Tornoe, C. W. Cu-Catalyzed Azide-Alkyne Cycloaddition. *Chem. Rev.* **2008**, *108,* 2952–3015.

(24) Ikeda, T.; Moriyama, S.; Kim, J. Imidazolium-Based Poly(Ionic Liquid)S with Poly(Ethylene Oxide) Main Chains: Effects of Spacer and Tail Structures on Ionic Conductivity. *J. Polym. Sci. A Polym. Chem.* **2016**, *54,* 2896–2906.

(25) Shaplov, A. S.; Ponkratov, D. O.; Vlasov, P. S.; Lozinskaya, E. I.; Komarova, L. I.; Malyshkina, I. A.; Vidal, F.; Nguyen, G. T. M.; Armand, M.; Wandrey, C.; Vygodskii, Y. S. Synthesis and Properties of Polymeric Analogs of Ionic Liquids. *Polym. Sci. Ser. B* **2013**, *55,* 122–138.

(26) Wang, J. H. H.; Colby, R. H. Exploring the Role of Ion Solvation in Ethylene Oxide Based Single-Ion Conducting Polyanions and Polycations. *Soft Matter* **2013**, *9,* 10275–10286.

(27) Macdonald, J. R. Theory of AC Space-Charge Polarization Effects in Photoconductors, Semiconductors, and Electrolytes. *Phys. Rev.* **1953**, *92,* 4–17.

(28) Coelho, R. On the Relaxation of a Space-Charge. *Rev. Phys. Appl.* **1983**, *18,* 137–146.

(29) Klein, R. J.; Zhang, S. H.; Dou, S.; Jones, B. H.; Colby, R. H.; Runt, J. Modeling Electrode Polarization in Dielectric Spectroscopy: Ion Mobility and Mobile Ion Concentration of Single-Ion Polymer Electrolytes. *J. Chem. Phys.* **2006**, *124*, 144903.

(30) Phiasivongsa, P.; Luehr, G.; Peng, G.; By, K.; Anik, S. T. Preparation of Prodrugs of Peptide Epoxy Ketone Protease Inhibitors. US20140100154 A1, 2014.

(31) Percec, V.; Leowanawat, P.; Sun, H. J.; Kulikov, O.; Nusbaum, C. D.; Tran, T. M.; Bertin, A.; Wilson, D. A.; Peterca, M.; Zhang, S. D.; Kamat, N. P.; Vargo, K.; Moock, D.; Johnston, E. D.; Hammer, D. A.; Pochan, D. J.; Chen, Y. C.; Chabre, Y. M.; Shiao, T. C.; Bergeron-Brlek, M.; Andre, S.; Roy, R.; Gabius, H. J.; Heiney, P. A. Modular Synthesis of Amphiphilic Janus Glycodendrimers and Their Self-Assembly into Glycodendrimersomes and Other Complex Architectures with Bioactivity to Biomedically Relevant Lectins. J. Am. Chem. Soc. 2013, 135, 9055–9077.

(32) Nielsen, M. M.; Dimitrov, I.; Takamuku, S.; Jannasch, P.; Jankova, K.; Hvilsted, S. Dendronized Polymer Architectures for Fuel Cell Membranes. *Fuel Cells* **2013**, *13,* 342–354.

(33) Shaplov, A. S.; Vlasov, P. S.; Armand, M.; Lozinskaya, E. I.; Ponkratov, D. O.; Malyshkina, I. A.; Vidal, F.; Okatova, O. V.; Pavlov, G. M.; Wandrey, C.; Godovikov, I. A.; Vygodskii, Y. S. Design and Synthesis of New Anionic "Polymeric Ionic Liquids" with High Charge Delocalization. *Polym. Chem.* **2011**, *2,* 2609–2618.

(34) Liu, D. A.; Zheng, Y. J.; Steffen, W.; Wagner, M.; Butt, H. J.; Ikeda, T. Glycidyl 4-Functionalized-1,2,3-Triazole Polymers. *Macromol. Chem. Phys.* **2013**, *214,* 56–61.

(35) Seno, K. I.; Kanaoka, S.; Aoshima, S. Synthesis and LCST-Type Phase Separation Behavior in Organic Solvents of Poly(Vinyl Ethers) with Pendant Imidazolium or Pyridinium Salts. *J. Polym. Sci. A Polym. Chem.* **2008**, *46,* 5724–5733.

(36) Men, Y. J.; Schlaad, H.; Yuan, J. Y. Cationic Poly(Ionic Liquid) with Tunable Lower Critical Solution Temperature-Type Phase Transition. *ACS Macro Lett.* **2013**, *2,* 456–459.

(37) Kohno, Y.; Saita, S.; Men, Y. J.; Yuan, J. Y.; Ohno, H. Thermoresponsive Polyelectrolytes Derived from Ionic Liquids. *Polym. Chem.* **2015**, *6,* 2163–2178.

(38) Bocharova, V.; Sokolov, A. P. Perspectives for Polymer Electrolytes: A View from Fundamentals of Ionic Conductivity. *Macromolecules* **2020**, *53,* 4141–4157.

(39) Gainaru, C.; Stacy, E. W.; Bocharova, V.; Gobet, M.; Holt, A. P.; Saito, T.; Greenbaum, S.; Sokolov, A. P. Mechanism of Conductivity Relaxation in Liquid and Polymeric Electrolytes: Direct Link between Conductivity and Diffusivity. *J. Phys. Chem. B* **2016**, *120,* 11074–11083.

(40) Kosters, J.; Schonhoff, M.; Stolwijk, N. A. Ion Transport Effects in a Solid Polymer Electrolyte Due to Salt Substitution and Addition Using an Ionic Liquid. *J. Phys. Chem. B* **2013**, *117,* 2527–2534.

(41) Hayamizu, K.; Tsuzuki, S.; Seki, S.; Umebayashi, Y. Nuclear Magnetic Resonance Studies on the Rotational and Translational Motions of Ionic Liquids Composed of 1-Ethyl-3-Methylimidazolium Cation and Bis(trifluoromethanesulfonyl)amide and Bis(fluorosulfonyl)amide Anions and Their Binary Systems Including Lithium Salts. *J. Chem. Phys.* **2011**, *135*, 084505.

(42) Hou, J. B.; Zhang, Z. Y.; Madsen, L. A. Cation/Anion Associations in Ionic Liquids Modulated by Hydration and Ionic Medium. *J. Phys. Chem. B* **2011**, *115,* 4576–4582.

(43) Ikeda, T.; Nagao, I.; Moriyama, S.; Kim, J. D. Synthesis and Characterization of Glycidyl-Polymer-Based Poly(Ionic Liquid)s: Highly Designable Polyelectrolytes with a Poly(Ethylene Glycol) Main Chain. *RSC Adv.* **2015**, *5*, 87940–87947.